Twelfth International Congress on Sound and Vibration

JUSTIFICATION OF THE IMAGE SOURCES IN RAY-TRACING METHOD

Vincent Martin[1] and Thomas Guignard[2]

[1]CNRS - Laboratoire de Mécanique Physique : 2, place de la Gare de Ceinture, F-78210 St-Cyr l'Ecole, France ; vmartin@ccr.jussieu.fr
[2]EPFL – Laboratoire d'Electromagnétisme et d'Acoustique : STI-ITOP-LEMA, Station 11, CH-1015 Lausanne, Switzerland ; thomas.guignard@epfl.ch

Abstract

This paper discusses the identification of the image sources commonly used in ray-tracing methods as terms of a series development of the integral solution. This more formal backing of an otherwise intuitive method not only helps understanding its implications on the resulted precision (notably through a simplification of the Huygens' principle) but also shows how the ray-tracing method could be enhanced by adding certain "invisible" sources.

I - INTRODUCTION

Modern acoustic ray-tracing methods rest upon specular reflection and the identification of image sources, from which the rays originate. These two assumptions are also the two shortcomings of the method: on the one hand, specular reflection is known to be imprecise (because it doesn't take into account the non-locality of the wave reflection) and on the other hand, the identification of the image sources is the result of a purely geometrical approach, which doesn't take into consideration diffraction phenomena. Even when the problem of specular reflection is solved (in test cases with perfectly reflecting walls), errors due to missing image sources can occur in nontrivial geometries, such as in the vicinity of an obtuse angle. The precision of the image sources method needs to be further examined. To this aim, it has been shown that the exact integral solution of a 2D acoustic problem, expressed as a series of terms, could be seen as the contribution of the different image sources (via a first approximation of the Huygens principle). Could the correspondence between the "exact" terms and the image sources be shown, the missing sources would appear and the method could therefore be refined.

II - FORMALISM

II-1 Integral representation on the boundaries and series development

Any comparison between acoustic fields obtained by the image source method and by boundary integral method needs as a preliminary to show the algorithm which usually chooses the image sources. The image issued from wall n originates by a mirror effect on that wall from a source, that could itself be the image from wall k. It is convenient to write it $S_{\underbrace{\ldots\ldots kn}_{l \text{ indices}}}$ to signify that it will give rise to l reflections from the actual source, the last one on the wall n, the previous one on the wall k, etc. For example, the source denoted S_5 is the image of the real source through wall 5, and source S_{53} is the image of source S_5 through wall 3. Its presence will show two reflections. This can happen only if the last reflection is liable to reach a point inside the domain. To clarify the view, Figure 1 presents a 2D domain made up of an angular sector defined by two semi-infinite straight lines, in fact two segment (of finite length). Six image sources will give rise to reflections. However to reach point P, only four image-sources are useful; only source S_{212} would give a reflected ray reaching point Q ; for R, three image source intervene.

By inspection of Figure 1, it appears that an image source plays a role, for point P for instance, if the ray from that source goes through wall n to reach P. In these conditions, source S_{212} is of no use for point Q as the ray from S_{212} does not go through wall Γ_2 to reach Q.

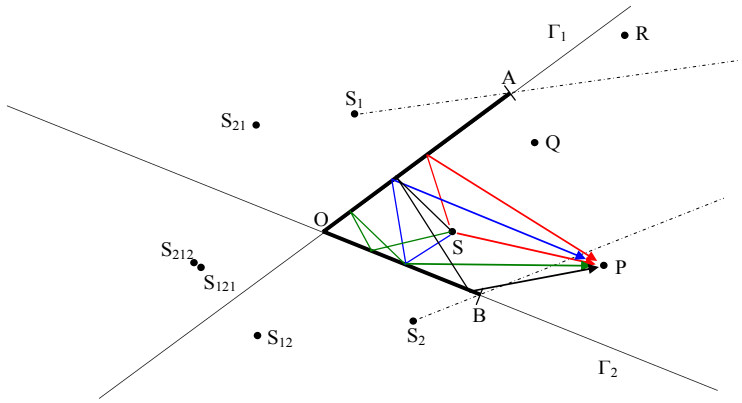

Figure 1 - Set of image sources liable to give rise to reflected rays for points in the angular sector ; set of rays (i.e., of sources) contributing to the calculation of the acoustic field at point P (figure from written lessons by V. Martin).

Having thus in mind the algorithm for determining the sources, the motivation of the present work arises from both diagrams on Figure 2. The sector is now defined by the semi-infinite straight lines Γ_1, and Γ_2. The configuration on the left leads to four sources (three images and the real source) and the validity of the field obtained at point Q_1 is not guaranteed. On the contrary, to the right, the only image source available leads to a doubt on the obtained field, as it is not expected that wall Γ_2 doesn't play any role at all (source S_1 reveals the presence of wall Γ_1 only).

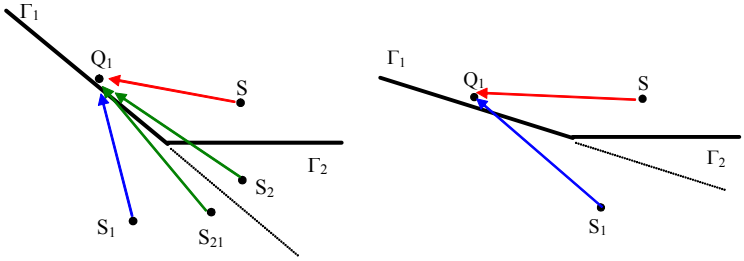

Figure 2 - The implementation of the algorithm for determining the useful image sources for point Q_1 results in three images to the left and only one to the right.

However, it is possible to enlighten the degree of precision of the field obtained by rays by comparing them to the exact solution given by the integral representation. In the 2D unbounded space, the Green function $\mathrm{G}(S,R)$ represents the field at point R emitted by a source located at S provided with a particular velocity. In the first diagram, the acoustic pressure from the rays would be expressed by

$$p_{ray}(Q_1) = \underbrace{\mathrm{G}(S,Q_1)}_{G_0(Q_1)} + \underbrace{\mathrm{G}(S_1,Q_1)}_{G_1(Q_1)} + \underbrace{\mathrm{G}(S_2,Q_1)+\mathrm{G}(S_{21},Q_1)}_{2\mathrm{G}(S_2,Q_1)=2G_2(Q_1)} \tag{1}$$

(implicitly, the amplitude of the source term on the right-hand side of Helmholtz equation is unity). On another side, since equality

$$2\,\mathrm{G}_0(Q_1) = \mathrm{G}_0(Q_1) + \mathrm{G}_1(Q_1) \tag{2}$$

is rigorous when $Q_1 \in \Gamma_1$ (it can be demonstrated), the exact solution on the walls resulting from the integral representation is

$$p(Q_1) = \mathrm{G}_0(Q_1) + \mathrm{G}_1(Q_1) + 2\int_{\Gamma_2} p(M)\,\partial_{n_M}\mathrm{G}(M,Q_1)\,dM \tag{3}$$

denoting thus $p(\Gamma_1)$ depending on $p(\Gamma_2)$; similarly for $p(Q_2)$. We are in presence of two integral equations for two unknown functions.

The formal discretized writing of the integral representation is noted

$$\underbrace{p(Q_1)}_{\mathbf{p_1}} = \underbrace{\mathrm{G}_0(Q_1)}_{\mathbf{g_0}(\Gamma_1)} + \underbrace{\mathrm{G}_1(Q_1)}_{\mathbf{g_1}(\Gamma_1)} + \underbrace{2\int_{\Gamma_2} p(M)\,\partial_{n_M}\mathrm{G}(M,Q_1)\,dM}_{2\mathbf{B}\cdot\mathbf{p_2}} \tag{4}$$

and similarly for $\mathbf{p_2}$. Thus

$$\begin{aligned}\mathbf{p_1} &= (\mathbf{I}-2\mathbf{B}\cdot 2\mathbf{C})^{-1}\cdot\left(\mathbf{g_0}(\Gamma_1)+\mathbf{g_1}(\Gamma_1)\right)+(\mathbf{I}-2\mathbf{B}\cdot 2\mathbf{C})^{-1}\cdot 2\mathbf{B}\cdot\left(\mathbf{g_0}(\Gamma_2)+\mathbf{g_2}(\Gamma_2)\right)\\ \mathbf{p_2} &= (\mathbf{I}-2\mathbf{C}\cdot 2\mathbf{B})^{-1}\cdot\left(\mathbf{g_0}(\Gamma_2)+\mathbf{g_2}(\Gamma_2)\right)+(\mathbf{I}-2\mathbf{C}\cdot 2\mathbf{B})^{-1}\cdot 2\mathbf{C}\cdot\left(\mathbf{g_0}(\Gamma_1)+\mathbf{g_1}(\Gamma_1)\right)\end{aligned} \tag{5}$$

Formally, developing in series would result in the expressions

$$\begin{aligned}\mathbf{p_1} &= \mathbf{g_0}(\Gamma_1)+\mathbf{g_1}(\Gamma_1)+2\mathbf{B}\cdot\left(\mathbf{g_0}(\Gamma_2)+\mathbf{g_2}(\Gamma_2)\right)+2\mathbf{B}\cdot 2\mathbf{C}\cdot\left(\mathbf{g_0}(\Gamma_1)+\mathbf{g_1}(\Gamma_1)\right)+\ldots\\ \mathbf{p}_2 &= \mathbf{g_0}(\Gamma_2)+\mathbf{g_2}(\Gamma_2)+2\mathbf{C}\cdot\left(\mathbf{g_0}(\Gamma_1)+\mathbf{g_1}(\Gamma_1)\right)+2\mathbf{C}\cdot 2\mathbf{B}\cdot\left(\mathbf{g_0}(\Gamma_2)+\mathbf{g_2}(\Gamma_2)\right)+\ldots\end{aligned} \tag{6}$$

Now, Huygens principle enacts that the emitted field from a source at a reception point is liable to be seen as the contribution of fictitious sources located on the wavefront between the source and the reception point. This assertion, qualitative at that step, is sufficient to try progressing toward an eventual correlation between the terms of the series and the image sources. Indeed, keeping an eye on $\mathbf{p_1}$, it is noticeable that $2\mathbf{B}\cdot\mathbf{g_0}(\Gamma_2)$ is the pressure radiated by S toward Γ_2 transferred to Γ_1

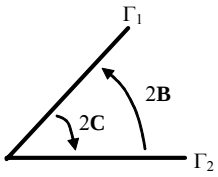

Figure 3 - Matrices 2B et 2C transfer respectively pressure on wall Γ_2 towards wall Γ_1 and inversely.

through the multiplication by $2\mathbf{B}$. It is also the pressure originating from S_2 on Γ_2 transferred to Γ_1, that is pressure from S_2 radiated to Γ_1 denoted $\mathbf{g_2}(\Gamma_1)$. This last deduction lacks rigor for the time being. In fact, it would be necessary to know the radiated pressure by S_2 on the whole (infinite) wall Γ_2 to assimilate the pressure transferred to points of Γ_1 to the one radiated there by S_2.

To this first reasoning, another one is added. Term $2\mathbf{B}\cdot\mathbf{g_2}(\Gamma_2)$ represents pressure due to S_2 on Γ_2 transferred to Γ_1 i.e. pressure from S_2 on Γ_1. It is also the pressure from to Γ_1 or $\mathbf{g_{21}}(\Gamma_1)$, with the same lack of rigor as written above. With both scheme of reasoning, it appears (terms of the same order are in brackets)

$$\begin{aligned}\mathbf{p_1} &= \left[\mathbf{g_0}(\Gamma_1)+\mathbf{g_1}(\Gamma_1)\right]+\left[\mathbf{g_2}(\Gamma_1)+\mathbf{g_{21}}(\Gamma_1)\right]+\left[\mathbf{g_{12}}(\Gamma_1)+\mathbf{g_{121}}(\Gamma_1)\right]+\ldots \\ \mathbf{p_2} &= \underbrace{\left[\mathbf{g_0}(\Gamma_2)+\mathbf{g_2}(\Gamma_2)\right]}_{0^{th}\text{ order terms}}+\underbrace{\left[\mathbf{g_1}(\Gamma_2)+\mathbf{g_{12}}(\Gamma_2)\right]}_{1^{st}\text{ order terms}}+\underbrace{\left[\mathbf{g_{21}}(\Gamma_2)+\mathbf{g_{212}}(\Gamma_2)\right]}_{2^{nd}\text{ order terms}}+\ldots\end{aligned} \qquad (7)$$

Remark on the order of importance of image-sources

To put the above formalism in relation with the diagram of motivation on Figure 2, we ought to conclude that the sources S_{12}, S_{121}, etc… are missing on the left configuration, and sources S_2, S_{21}, etc… for the configuration on the right. Moreover, taking into account the natural order of terms in the series for $\mathbf{p_1}$, the first source that ought to be added would be S_{12}, which is not suitable since it is inside the domain. On the right, source S_2 ought to be considered next. The algorithm for determining the sources would take it into account, were wall 2 lengthened towards the left. Finally, the order of sources for $\mathbf{p_1}$ is not the same for $\mathbf{p_2}$.

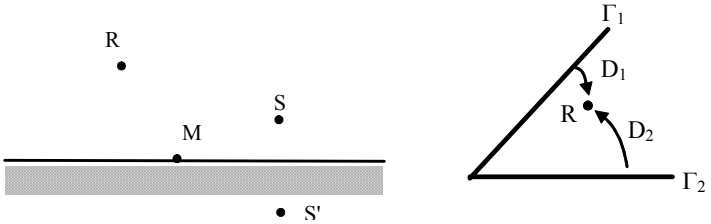

Figure 4 - Left : elementary configuration with a reflection on the wall; Right : transfer of pressures from the wall toward the inside of the domain.

II-2 Integral representation inside the domain and series development

In the elementary configuration of figure 4, to the left, pressure at point R is expressed by

$$p(R) = \mathrm{G}_0(R) + \underbrace{\int_{\Gamma} p(M)\partial_{n_M}\,\mathrm{G}(M,R)dM}_{\text{contribution from } S',\text{ or } \mathrm{G}'(R)} \qquad (8)$$

with

$$p(M) = \mathrm{G}(S, M) + \mathrm{G}(S', M) = 2\,\mathrm{G}(S', M) \tag{9}$$

thus leading to

$$\mathbf{p} = \mathbf{g}(\Omega) + \mathbf{D}_\infty \cdot 2\mathbf{g}'(\Gamma) = \mathbf{g}(\Omega) + \mathbf{D}_\infty \cdot \mathbf{p}(\Gamma) \tag{10}$$

For the configuration under study here, we write similarly

$$\mathbf{p} = \mathbf{g_0}(\Omega) + \mathbf{D_1} \cdot \mathbf{p_1} + \mathbf{D_2} \cdot \mathbf{p_2} \tag{11}$$

During the analysis of the series development to obtain the source contribution, it appears that terms are accounted by pairs. Indeed, the formulation is also

$$\begin{aligned}
\mathbf{p} = \mathbf{g_0}(\Omega) \;+\; & \mathbf{D_1}.(\underbrace{\mathbf{g_0}(\Gamma_1) + \mathbf{g_1}(\Gamma_1)}_{2\,\mathbf{g_1}(\Gamma_1)} + \underbrace{\mathbf{g_{12}}(\Gamma_1) + \mathbf{g_{121}}(\Gamma_1)}_{2\,\mathbf{g_{121}}(\Gamma_1)} + \underbrace{\mathbf{g_{1212}}(\Gamma_1) + \mathbf{g_{12121}}(\Gamma_1)}_{2\,\mathbf{g_{12121}}(\Gamma_1)} + \ldots) \\
+\; & \mathbf{D_1}.(\underbrace{\mathbf{g_2}(\Gamma_1) + \mathbf{g_{21}}(\Gamma_1)}_{2\,\mathbf{g_{21}}(\Gamma_1)} + \underbrace{\mathbf{g_{212}}(\Gamma_1) + \mathbf{g_{2121}}(\Gamma_1)}_{2\,\mathbf{g_{2121}}(\Gamma_1)} + \underbrace{\mathbf{g_{21212}}(\Gamma_1) + \ldots}_{2\,\mathbf{g_{21212}}(\Gamma_1)} + \ldots) \\
+\; & \mathbf{D_2}.(\underbrace{\mathbf{g_0}(\Gamma_2) + \mathbf{g_2}(\Gamma_2)}_{2\,\mathbf{g_2}(\Gamma_2)} + \underbrace{\mathbf{g_{21}}(\Gamma_2) + \mathbf{g_{212}}(\Gamma_2)}_{2\,\mathbf{g_{212}}(\Gamma_2)} + \underbrace{\mathbf{g_{21212}}(\Gamma_2) + \mathbf{g_{212121}}(\Gamma_2)}_{2\,\mathbf{g_{212121}}(\Gamma_2)} + \ldots) \\
+\; & \mathbf{D_2}.(\underbrace{\mathbf{g_1}(\Gamma_2) + \mathbf{g_{12}}(\Gamma_2)}_{2\,\mathbf{g_{12}}(\Gamma_2)} + \underbrace{\mathbf{g_{121}}(\Gamma_2) + \mathbf{g_{1212}}(\Gamma_2)}_{2\,\mathbf{g_{1212}}(\Gamma_2)} + \underbrace{\mathbf{g_{12121}}(\Gamma_2) + \mathbf{g_{121212}}(\Gamma_2)}_{2\,\mathbf{g_{121212}}(\Gamma_2)} + \ldots)
\end{aligned} \tag{12}$$

Transferring the pressures from the walls toward the domain through $\mathbf{D}_1$ and $\mathbf{D}_2$ leads to

$$\mathbf{p} = \mathbf{g}_0(\Omega) + \mathbf{g}_1(\Omega) + \mathbf{g}_2(\Omega) + \mathbf{g}_{12}(\Omega) + \mathbf{g}_{21}(\Omega) + \mathbf{g}_{121}(\Omega) + \mathbf{g}_{212}(\Omega) + \mathbf{g}_{1212}(\Omega) + \ldots \tag{13}$$

where assembling terms by pairs always takes into account terms of the same order in the series revealing the pressures on the walls .

III - NUMERICAL EXPERIMENTS

As said in Section II, the reasoning correlating the terms of the series development and the image sources could lack rigor. An analysis of this reasoning will sooner or later prove necessary, but numerical experiments can yield faster results and provide a factual confirmation of the interpretation presented here.

All the experiments presented therein are made in a situation composed by two perfectly reflecting walls Γ_1 and Γ_2, having an angle of θ between them. The pressure is computed on both walls. In the following figures, the solution obtained by the image sources method is compared with the corresponding terms of the series development. The reference solution in all cases is computed with the integral method.

Seeking a way to observe if there is a correspondence between the terms of the series development and the image sources for the computation of the pressure on the walls, the first test comes from an intuitive consideration. For a small angle θ (acute), a great number of reflections can occur between both walls, so a great number of image sources is expected. For $\theta > \pi/2$ (obtuse), a small number of sources should intervene. It could be that the number of image sources is a monotonous function of the angle, so there should be a rapid convergence of the series for obtuse angles and a slow one for acute angles.

To verify this assertion, a distance between the exact solution and the solution

obtained with a number N_t of terms of the series development or obtained with a number N_s of image sources is defined as

$$d(N_t) = \int_{\Gamma_1} \left| p_{series}(N_t, \mathbf{x}) - p_{exact}(\mathbf{x}) \right|^2 d\mathbf{x} \text{ and } d(N_s) = \int_{\Gamma_1} \left| p_{sources}(N_s, \mathbf{x}) - p_{exact}(\mathbf{x}) \right|^2 d\mathbf{x} \quad (14)$$

For an acute angle, the image choice algorithm shows that all image sources are visible for the wall pressure. Figure 5 shows that the convergence curves of both the ray-tracing and series development solutions are closely related and verify the fact that the convergence is faster for wider angles. The correspondence between the terms of the series development and the image sources can therefore be deepened. Furthermore, the extra terms of the series development (those without an image source equivalent) appear to be either negligible or null, which confirms the theory but cannot be explained yet. The results corresponding to the 1/4-infinite case ($\theta = \pi/2$) will not be discussed as they confirm the validity of the method.

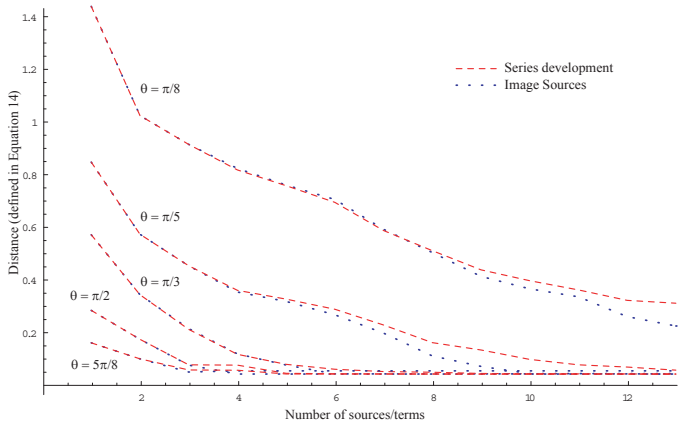

Figure 5 - Convergence speed as function of aperture angle θ.

For an acute angle θ, the interpretation of the series development proves therefore correct in a first approximation and hints to a formal justification for the image sources method, but offers no improvement over this method. On the contrary for obtuse angles, one can show the effects of adding the "supplementary" sources, coming from the terms of the series development without a "real" corresponding image source ("invisible" source as shown in Figure 2). To show the impact of this extra source, two situations, showing characteristic features of the method, are displayed here.

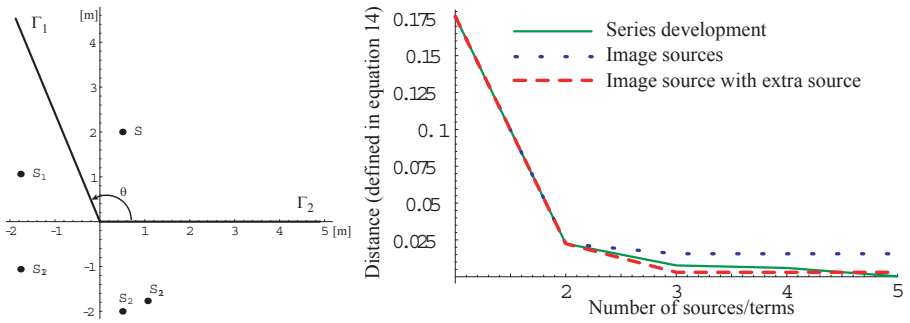

Figure 6 - Situation A and convergence on wall Γ_1.

Figure 6 shows an increase in precision when an extra source (in that case S_2) is

added. For another situation, however, Figure 7 seems to show that adding a source can indeed worsen the solution. This puts the distance as defined in (14) into question and leads to the observation of the "strong convergence", that is the comparison between the actual pressure levels obtained by both methods.

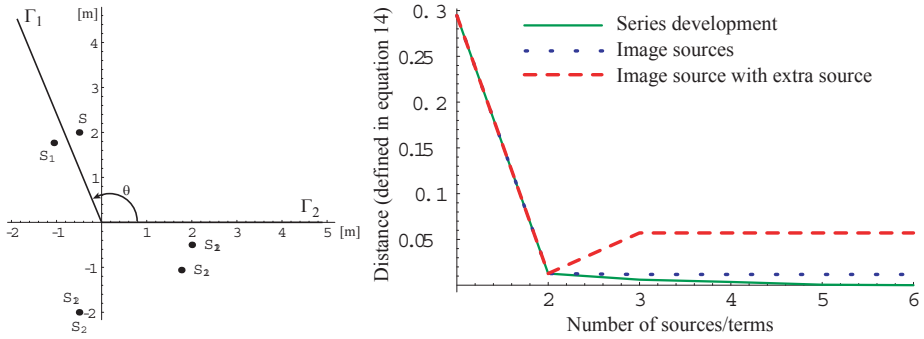

Figure 7 – Situation B and convergence on wall Γ_1.

Instead of observing a mean value between the exact solution and the computed one, the actual pressure level on each point of the wall is observed.

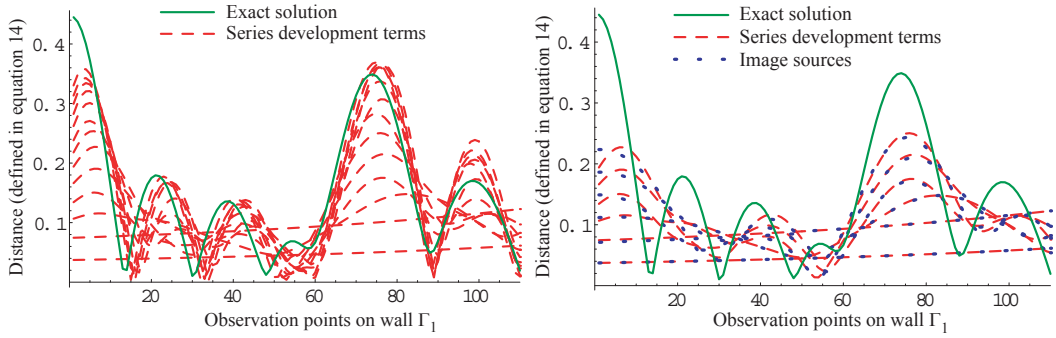

Figure 8 - Strong convergence: Left, convergence of the series development terms towards the exact solution; Right, contribution of the first 6 terms of the series development and corresponding image sources.

Figure 8 shows the strong convergence in the case of θ acute. The terms of the series development can bee seen converging towards the exact solution. A more detailed view shows the first 6 terms and their corresponding image sources. An almost perfect coherence between the terms and the sources can be observerd. This is expected for the first two terms, since they are conceptually identical, but the coherence of the higher terms is significant of the validity of the interpretation.

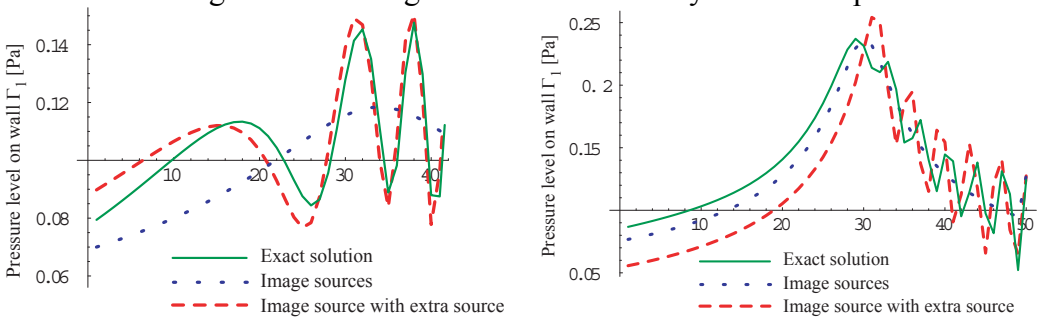

Figure 9 - Effect of an "invisible" source Right: Situation A, Left: Situation B

Observing the pressure level on the walls ("strong convergence") for cases with an

obtuse angle θ (situations A and B depicted in Figure 6 and Figure 7) shows the enhancement bought by adding an extra "invisible" source (in that case S_2). The oscillatory behavior of the wall pressure does not appear if only the "visible" sources are used. This valuable information is added when an extra source is used (which was not shown when only observing the weak convergence, as in Figure 7).

IV - CONCLUSION

It is then shown that adding an extra source, hinted by the interpretation as image sources of the series development terms, actually adds valuable information, be it in the sense of the weak convergence or strong convergence in the most cases. Figure 9 (right) shows however that the extra source, when actually adding missing information, can also show some divergence (in this case a "phase shift").

This divergence can be even greater in specific configurations if observing the pressure inside the cavity (and not on the walls as presented here), which brings the question of defining "influence zones" where extra sources should be added. Indeed, if on the one hand it is easy to determine the source to be added when dealing with wall pressure, on the other hand, inside the cavity, the order of the image sources corresponding to the series development terms as presented in (12) strongly depends on the relative strength of the terms coming from each wall. The next step of the method is therefore to define these zones and their influence on the choice of the most important extra source to be added.

REFERENCES

[1] T. Courtois, V. Martin, "Spectral quality of acoustic predictions obtained by the ray method in coupled two-dimensional damped cavities", J. Sound Vib., 270, 259-278 (2004)

[2] J. Allen, D.A. Berkley, "Image method for efficiently simulating small-rooms acoustics", J. Acoust. Soc. Am., 65, 943-950 (1979)

[3] H. Kuttruf, *Room Acoustics*. (4th edition, Spon Press, London, 2000)

Acknowledgment

This research is supported by the Swiss CTI 6604.2 and 7294.1 EUS-IW projects under European label EUREKA 2790. It is done in collaboration with and upon an initial proposition from *RIETER Automotive Management Corp.* in Winterthur, Switzerland.